INCLUSIVE ELECTRON SCATTERING FROM NUCLEI: y SCALING AND FINAL STATE INTERACTION

Dino FARALLI

Department of Physics, University of Perugia, and

Istituto Nazionale di Fisica Nucleare, Sezione di Perugia

Via A. Pascoli, I–06100 Perugia, Italy

Claudio CIOFI degli ATTI * and Geoffrey B. WEST

Theoretical Division, T-8, MS B285, Los Alamos National Laboratory

Los Alamos, NM 87545, USA .

(October 27, 1999)

Abstract

The recent TJLAB experimental data on inclusive electron scattering at high momentum transfer from complex nuclei are analyzed in terms of y scaling, taking into account the final state interaction (FSI) of the struck, off-shell nucleon. It is shown that at large negative values of y ($x > 1$), the Q^2 dependence of the FSI is mostly driven by the *elastic* nucleon-nucleon cross section, and that, as a result, the scaling function decreases with Q^2, in agreement with experimental data.

---

*Permanent address: Department of Physics, University of Perugia, and Istituto Nazionale di Fisica Nucleare, Sezione di Perugia, Via A. Pascoli, I–06100 Perugia, Italy .

I. INTRODUCTION

The recently released TJNAF E89-008 experimental data on inclusive electron scattering $A(e,e')X$ at $x > 1$ ($x = \frac{Q^2}{2M\nu}$ is the Bjorken scaling variable) and high momentum transfer [1] could provide relevant information on nucleon momentum distributions in nuclei and the mechanism of final state interactions in inclusive processes. In this contribution, these data are analyzed by calculating both the cross sections and the y-scaling functions, using, in the latter case, a recently proposed new approach [2]. The effects of FSI will be considered, stressing the relevant role played by the off-shell kinematics for the struck nucleon before its rescattering from spectator nucleons in the medium.

II. THE INCLUSIVE CROSS SECTION

The inclusive electron-nucleus cross section can be written in the following general form:

$$\frac{d^2\sigma_{eA}}{d\Omega d\nu} = \sigma_{Mott}\left[W_2^A(Q^2,\nu) + 2\tan^2(\theta/2)W_1^A(Q^2,\nu)\right] \tag{1}$$

where $Q^2 = \mathbf{q}^2 - \nu^2$ is the four-momentum transfer squared, and σ_{Mott} the Mott cross section. In plane wave impulse approximation (PWIA), the nuclear structure functions $W_{1,2}$ are given by

$$W_i^A(Q^2,\nu) = \sum_{N=1}^{A}\int d\mathbf{k}\int dE\, P^N(k,E)\left[C_i W_1^N(Q^2,\nu\prime) + D_i W_2^N(Q^2,\nu\prime)\right] \tag{2}$$

where $i = \{1,2\}$, $W_{1(2)}^N$ are the nucleon structure functions, C_i and D_i are some kinematics factors, $\nu' = (p\cdot Q)/M$ where p is the four-momentum of the struck off-shell nucleon, and $P^N(k,E)$ its *spectral function*; we denote the three-momentum of the struck nucleon by $k = |\mathbf{p}|$ and its removal energy by $E = E_{min} + E^*_{A-1}$ where $E_{min} = M_{A-1} + M - M_A$.

We have calculated the cross section (1) both in the quasi-elastic and inelastic regions using the experimental nucleon structure functions and the spectral function from Ref. [3]. The PWIA results for ^{56}Fe are represented in Fig. 1 by the dotted curve, which is the

sum of the quasi-elastic (short dashes) and inelastic (long dashes) contributions. The well-known result, that the PWIA underestimates the cross section at low values of ν ($x > 1$) is shown to hold true for the new data. We have included the FSI of the struck nucleon using the method of Ref. [3]. The results are shown by the full curve where it is seen that the agreement with the experimental data is satisfactory. More details on the calculation of the FSI will be given in Section IV. At $x > 1$, the contribution from inelastic channels is always very small, the dominant process being quasi-elastic scattering; this therefore justifies an analysis of the data in terms of y-scaling.

III. QUASI-ELASTIC SCATTERING AND Y-SCALING

In PWIA the quasi-elastic cross-section is given by

$$\frac{d^2\sigma_{eA}^{qe}}{d\Omega d\nu} = 2\pi \sum_{N=1}^{A} \int_{E_{min}}^{E_{max}(q,\nu)} dE \int_{k_{min}(q,\nu,E)}^{k_{max}(q,\nu,E)} k\, dk\, P_A^N(k,E)\sigma_{eN}(Q^2,\nu')\frac{E_p}{q} \tag{3}$$

where $E_p = \sqrt{M^2 + (\mathbf{k}+\mathbf{q})^2}$ is the *on shell* energy of the struck nucleon after photon absorption , $q = |\mathbf{q}|$ and σ_{eN} is the elastic electron-nucleon cross section. The integration limits in (3) are determined from energy conservation:

$$\nu + M_A = \sqrt{M^2 + (\mathbf{k}+\mathbf{q})^2} + \sqrt{M_{A-1}^{*2} + \mathbf{k^2}}. \tag{4}$$

where $M_{A-1}^* = M_{A-1} + E_{A-1}^*$ is the mass of the excited $(A-1)$ system. At large values of the momentum transfer, the following relation holds

$$\frac{d^2\sigma_{eA}^{qe}}{d\Omega d\nu} = F_A(q,\nu)\left[(Z\sigma_{ep} + N\sigma_{en})\frac{E_p}{q}\right]_{(k=k_{min},E=E_{min})} \tag{5}$$

where the nuclear structure function, $F_A(q,\nu)$, is given by

$$F_A(q,\nu) = 2\pi \int_{E_{min}}^{E_{max}(q,\nu)} dE \int_{k_{min}(q,\nu,E)}^{k_{max}(q,\nu,E)} k\, dk\, P(k,E) \tag{6}$$

(assuming $P^p = P^N \equiv P$). In analyzing quasi-elastic scattering in terms of y scaling [4] a new variable $y = y(q,\nu)$ is introduced and Eq. (6) expressed in terms of q and y rather than q and ν.

The most commonly used scaling variable [1] is obtained [5] starting from relativistic energy conservation, Eq. (4), and setting $k = y$, $\frac{\mathbf{k}\cdot\mathbf{q}}{kq} = 1$, and, most importantly, the excitation energy $E^*_{A-1} = 0$; in other words, y is obtained from the following equation:

$$\nu + M_A = [M^2_{A-1} + y^2]^{1/2} + [M^2 + (y+q)^2]^{1/2} \tag{7}$$

In this case, y therefore represents the longitudinal momentum of a nucleon having the minimum removal energy ($E = E_{min}$, i.e. $E^*_{A-1} = 0$). It can be shown [5] that, at high values of q, $E_{max} \simeq \infty$ and $k_{min} \simeq |y - (E - E_{min})|$, so that Eq. (6) reduces to

$$F_A(q,y) \rightarrow f_A(y) = 2\pi \int_{E_{min}}^{\infty} dE \int_{|y-(E-E_{min})|}^{\infty} k\, dk\, P^N_A(k,E) \tag{8}$$

explicitly showing scaling in y. By defining an experimental scaling function

$$F^{exp}_A(y,q) = \frac{(\frac{d^2\sigma^{qe}_{eA}}{d\Omega d\nu})^{exp}}{(Z\sigma_{ep} + N\sigma_{en})\frac{E_p}{q}} \tag{9}$$

and comparing it with the theoretical expression, Eq. (6), important information can in principle be obtained. For example, from deviations between Eqs. (6) and (9), one can learn about FSI whilst, if scaling is observed, one can learn about the nucleon spectral function, $P^N_A(k,E)$. In practice, binding effects, i.e. the dependence of k_{min} upon E (and, therefore, E^*_{A-1}), do not permit a direct relationship between $F_A(y)$ and the longitudinal momentum distributions given by

$$f_A(y) = 2\pi \int_{|y|}^{\infty} k\, dk\, n_A(k) \tag{10}$$

where $n_A(k) = \int_{E_{min}}^{\infty} dE P_A(k,E)$ is the nucleon momentum distribution. Even at high momentum transfer, the contribution of FSI can "scale" due to the constant value of the total NN cross section, thereby confusing a direct extraction of $n_A(k)$ [7]. Moreover it should be pointed out that, when expressed in term of the usual scaling variable, y, a comparison between experimental and theoretical scaling functions requires knowledge of

[1] For other types of scaling variables see [6]

the nucleon spectral function. This is difficult to calculate theoretically; on the other hand, theoretical knowledge of nucleon momentum distributions, $n_A(k)$, is rather well known, although experimentally it is very poor. There are, therefore, excellent reasons to justify an approach to y-scaling based on longitudinal momentum distributions, $f_A(y)$ (Eq. 10), rather than the asymptotic scaling function, Eq. (8). Apart from the trivial case of the deuteron, for which, by definition, $F_D(y) = f_D(y)$, the problem for complex nuclei is that the final spectator $(A-1)$ system can be left in all possible excited states, including the continuum. For this reason, the scaling variable defined by Eq. (7) can only be identified with the longitudinal momentum for weakly bound, shell model nucleons (where $E^*_{A-1} \simeq 0 - 20MeV$) but not for strongly bound, correlated nucleons (where $E^*_{A-1} \sim 50 - 200MeV$), whose contribution almost entirely saturates the scaling function at large values of y. Since the definition of the scaling variable is not unique, it is prudent to incorporate the most important dynamical effects, such as binding corrections, into its definition in order to establish a global link between experimental data and longitudinal momentum components. With this in mind we recently introduced such a scaling variable which has, to a large extent, the desired property of equally well representing longitudinal momenta of both weakly and strongly bound nucleons [2]. It is based upon the idea of effectively including in Eq. (7) the excitation energy of the $(A-1)$ system due to nucleon-nucleon correlations. This is given by [3,8]

$$E^*_{A-1}(\mathbf{k}) = \frac{A-2}{A-1}\frac{1}{2M}[\mathbf{k} - \frac{A-1}{A-2}\mathbf{K}_{CM}]^2 \tag{11}$$

where $\mathbf{k}$ is the relative momentum of a correlated pair and $\mathbf{K}_{CM}$ its CM momentum. This is in good agreement with results of many-body calculations for nuclei ranging from ^3He to nuclear matter [9]. We have evaluated the expectation value of Eq. (11) using realistic spectral functions obtaining [2]

[2]This is slightly different from the form given in ref. [3] and used in ref. [2] where a term quadratic in $\mathbf{k}$ was used instead of $c_A|\mathbf{k}|$; both forms are equally well acceptable.

$$< E^*_{A-1}(k) > \simeq \frac{A-2}{A-1}\frac{1}{2M}\mathbf{k}^2 + b_A - c_A|\mathbf{k}| \tag{12}$$

The parameters b_A and c_A, which result from the CM motion of the pair, have values ranging from $17MeV$ to $43MeV$ and 6.00×10^{-2} to 8.00×10^{-2}, for ^3He and nuclear matter, respectively. The idea was, therefore, to obtain the scaling variable by using this in the energy conservation equation, Eq. (4), thereby obtaining:

$$\nu + M_A = [(M_{A-2} + M + E^*_{A-1}(y))^2 + y^2]^{1/2} + [M^2 + (y+q)^2]^{1/2} \tag{13}$$

In order to ensure a smooth transition between the high and the low values of y, we shift the arbitrary scale of $< E^*_{A-1}(k) >$ in Eq. (12) by the average shell-model removal energy, $< E_{gr} >$: $< E^*_{A-1}(k) > \rightarrow < E^*_{A-1}(k) > - < E_{gr} >$. Note that $< E_{gr} >$ is not a free parameter since it is obtained from the Koltun sum rule. Furthermore, we use in Eq. (12) the relativistic form $\sqrt{M^2+\mathbf{k}^2} - M$ in place of $\frac{1}{2M}\mathbf{k}^2$.

For a heavy nucleus, where $M_{A-2} + M + E^*_{A-1}(y) \gg y$, the equation defining the new scaling variable therefore becomes

$$\sqrt{M^2+(y+q)^2} + \sqrt{M^2+y^2} + c_A y = \nu + M - E_{th} - b_A + < E_{gr} > \tag{14}$$

where $E_{th} = M_{A-2} + 2M - M_A$. Disregarding terms of order ${c_A}^2$ and c_A/q, Eq. (14) can be solved to obtain the new scaling variable in the form[3]

$$y_{CW} = -\frac{\tilde{q}}{2} + \left[\frac{\tilde{q}^2}{4} - \frac{4{\nu_A}^2M^2 - {\mathrm{W_A}}^4}{4\,{\mathrm{W_A}}^2}\right]^{1/2} \tag{15}$$

where $\nu_A = \nu + 2M - E_{th} - b_A + < E_{gr} >$, $\tilde{q} = q + c_A\nu_A$ and ${\mathrm{W_A}}^2 \equiv \nu_{\mathrm{A}}^2 - \mathrm{q}^2$.

It is worth emphasizing that, at low values of y, the usual scaling variable is recovered, $y_{CW} \simeq y$; indeed, y can be obtained from Eq. (15) as the limiting case where $b_A = c_A = < E_{gr} >= 0$. Furthermore, for the deuteron ($A = D$), $b_D = c_D = E_{gr} = 0$, $E_{th} = |\epsilon_D| =$

---

[3]These approximations, including the use of the relativistic form in Eq. (12), have been checked numerically and found to be very good ones in all kinematical regions of interest.

$2.225MeV$, $\nu_D = \nu + M_D$, $\tilde{q} = q$, and ${\rm W_A}^2 \equiv \nu_{\rm D}^2 - {\rm q}^2 = (-{\rm Q}^2 + {\rm M_D^2} + 2{\rm M_D}\nu)$, leading to the usual deuteron scaling variable $y_{CW} = y_D = -\frac{q}{2} + \left[\frac{q^2}{4} - \frac{4\nu_D^2 M^2 - {\rm W_D}^4}{4{\rm W_D}^2}\right]^{1/2}$. The use of y_{CW} instead of the usual y has the following advantages:

1. Since, at large values of q, the limits on the integrations in Eq. (6), $E_{max} \simeq E_{min} \simeq \infty$ and $k_{min}| \simeq y_{CW}|$ (instead of $k_{min} = |y - (E - E_{min})|$), the asymptotic scaling function when expressed as a function of y_{CW}, directly measures the longitudinal momentum distributions:

$$F_A(y_{CW}) \simeq f_A(y_{CW}) = 2\pi \int\limits_{|y_{CW}|}^{\infty} k\, dk\, n_A(k) \tag{16}$$

   Thus, plotting the data in terms of y_{CW} can provide direct access to the nucleon momentum distributions.

2. Since many body calculations [9] show that at high momenta, $k \geq 1.5 - 2fm^{-1}$, all nuclear momentum distributions are simply rescaled versions of the deuteron,

$$n_A(k) \cong C_A n_D(k) \tag{17}$$

   where C_A is a constant, one should also expect

$$F_A(q, y_{CW}) \cong C_A F_D(q, y_{CW}) \tag{18}$$

   On the other hand no such proportionality is expected between $F_A(q, y)$ and $F_D(q, y)$.

3. By eliminating binding effects, scaling violations observed in the experimental data, Eq. (9), can thereby be ascribed to the FSI, allowing a relatively clean separation between the two scale violating effects.

In order to check the validity of the above points, we show in Figs. 2 and 3 the experimental scaling functions for $A = 2, 4$ and 56, plotted in terms of the old and new scaling variables, respectively. It can be seen from Fig. 2 that the scaling functions, $F_A^{exp}(y, q)$ for $A = 4$ and 56, do not exhibit any simple proportionality to the deuteron scaling function

at large values of $|y|$, in contrast to the case of $F_A^{exp}(y_{CW}, q)$, shown in Fig. 3, which agrees remarkably well with the predictions of Eq. (18). The Q^2-dependence of $F_A^{exp}(y_{CW}, q)$, is shown in Figs. 4 and 5; in the latter figure we show the same scaling function divided by the constant C_A of Eq. (17), taken refs. [3,9].

IV. THE FINAL STATE INTERACTION

Figs. 4 and 5 show an approach to scaling from above and represent a clear signature of the effects of FSI. These were taken into account by a method [10] similar to the one used in Ref. [3]: both the rescattering of the struck nucleon via an optical potential generated by the shell model $(A-1)$ spectator system, as well as the two-nucleon rescattering in the final state when the struck nucleon is a partner of a correlated pair, were taken into account. The results are exhibited in Fig. 6 by the continuous line, while the dashed line represents the PWIA results and the dotted line the longitudinal momentum distributions. The following remarks are in order:

1. At high Q^2 the PWIA result is very similar to $f_A(y_{CW})$, as expected from Eq. (16). This is in marked contrast to what happens in the usual approach to y-scaling (cf. Fig. 2);

2. The calculated FSI *decreases* with Q^2, *approaching* the PWIA limit from above and, more importantly, agrees fairly well with the trend of the data.

The latter point requires specific comments, for it is a common belief that at high Q^2 FSI should be governed by the total nucleon-nucleon (NN) cross section which exhibits a constant behaviour for $p_N \geq 1.2 GeV/c$, where p_N is the lab momentum of the incident nucleon (see ref. [11]). In treating this point a crucial role is played by the four-momentum, p', of the struck nucleon after the absorption of the virtual photon. The usual procedure is to approximate its kinetic energy before rescattering by

$$T_q = E_q - M = \sqrt{q^2 + M^2} - M \simeq \frac{Q^2}{2M} \tag{19}$$

Such an approximation should be reasonable for $y \simeq 0$ ($x \simeq 1$), where the struck nucleon in the final state can be regarded as quasi-free (almost on shell, $p_1^2 \simeq M^2$). It should, however, be questioned at high negative values of y ($x \gg 1$), where, after absorbing the photon, the struck nucleon is far off-shell with invariant mass

$$p_1^2 \simeq M^2 + Q^2(\frac{1}{x} - 1) - \mathbf{k}^2 - 2k_L|\mathbf{q}| \tag{20}$$

where $k_L \equiv \hat{q}|\mathbf{k}|$. As a result, one has to consider the nucleon-nucleon cross section for a far-off-shell incident nucleon. This is a very difficult task. However, at the very least, one should consider off-shell kinematics. In such a case, the CM kinetic energy, T_{off}, of a two-nucleon pair after one nucleon has been struck by the virtual photon but before it rescatters from a spectator nucleon is, at large negative y ($x \gg 1$), *less* than the inelastic threshold ($= m_\pi$) . Thus, it is mostly the *elastic* NN cross section, which *decreases* with energy, that must be used rather than the constant total NN cross section.

V. EXTRACTION OF THE NUCLEON MOMENTUM DISTRIBUTIONS

Given the approach of the scaling function $F_A(y_{CW}, q)$ to the PWIA result exhibited in Figs. 4-7, the longitudinal momentum distribution can be extracted from the experimental data without the uncertainties associated with the subtraction of the so called binding correction (see Refs. [5], [6]). The example of ^{56}Fe is given in Fig. 8. By taking the derivative of $f(y_{CW})$ the nucleon momentum distributions $n(k)$ can be obtained.

VI. ACKNOWLEDGMENTS

CCdA and GBW acknowledge the hospitality of the Santa Fe Institute where part of this work was completed.

REFERENCES

[1] J. Arrington *et al* Phys. Rev. Lett. **82**, 2056 (1999).

[2] C. Ciofi degli Atti and G. B. West, Phys. Lett. C**53**, 1686 (1999).

[3] C. Ciofi degli Atti, S. Simula, Phys. Rev. C**53**, 1686 (1996).

[4] G. B. West, Phys. Rep. **18**, 263 (1975).
G. B. West, "New aspects on nuclear dynamics", Edited by J.H. Koch and K.A. de Witt-Huberts, Plenum Publ. Corp., (1989).

[5] C. Ciofi degli Atti, E. Pace and G. Salme, Phys. Rev. C**43**, 1155 (1991) and references quoted therein.

[6] A. Rinat, these Proceeding and references quoted therein.

[7] X. Ji and R. D. McKewon, Phys. Letts. **236**,130, (1990).

[8] L. L. Frankfurt and M. I. Strikman, Phys. Rep. **160**, 235, (1988).

[9] R. Schiavilla, V. R. Pandharipande and R. B. Wiringa, Nucl. Phys. A**449**, 219 (1986).

[10] C. Ciofi degli Atti, D. Faralli and G. B. West, in preparation.

[11] A. Baldini *et al* in "Total Cross Sections for Reactions of High Energy Particles", Ed. H. Schopper, Springer-Verlag, Berlin, 1987.

FIGURES

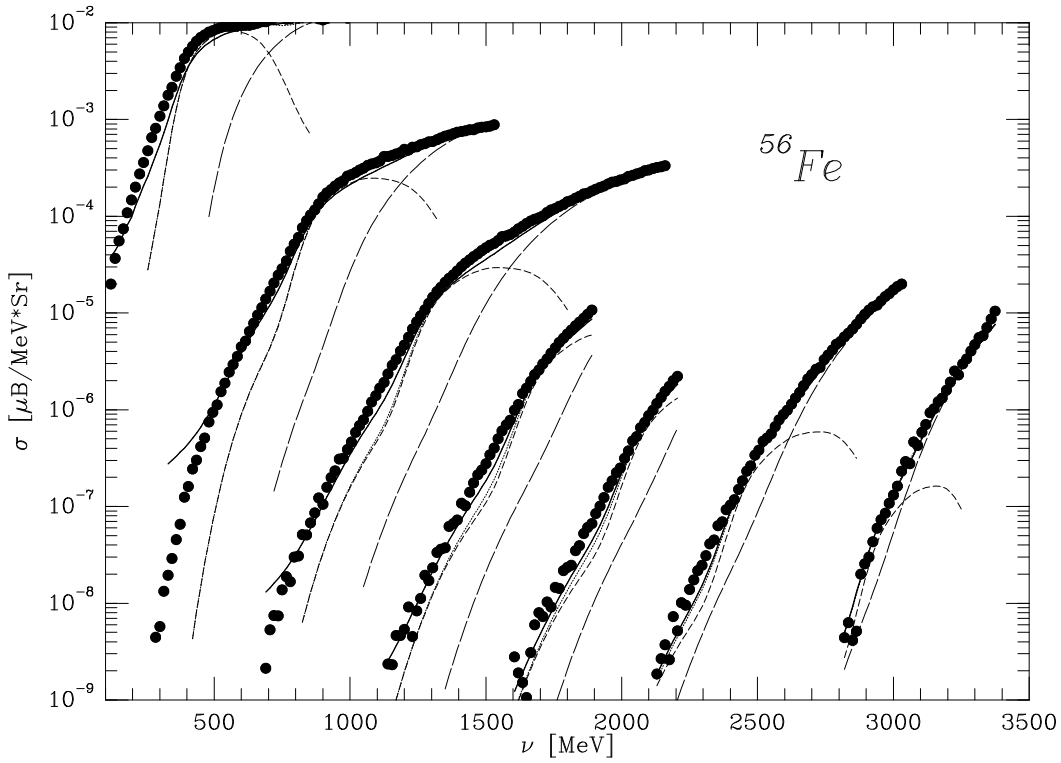

FIG. 1. The experimental data from Ref. 1 for ^{56}Fe (solid circles) compared to theoretical calculations. *Short-dashes*: quasi-elastic PWIA; *Long-dashes*: inelastic PWIA; *Dots*: sum of quasi-elastic and inelastic PWIA. The continuous line includes the effects of FSI. The various sets of experimental data correspond to different values of the scattering angle θ, ranging from 15^o to 74^o, from left to right .

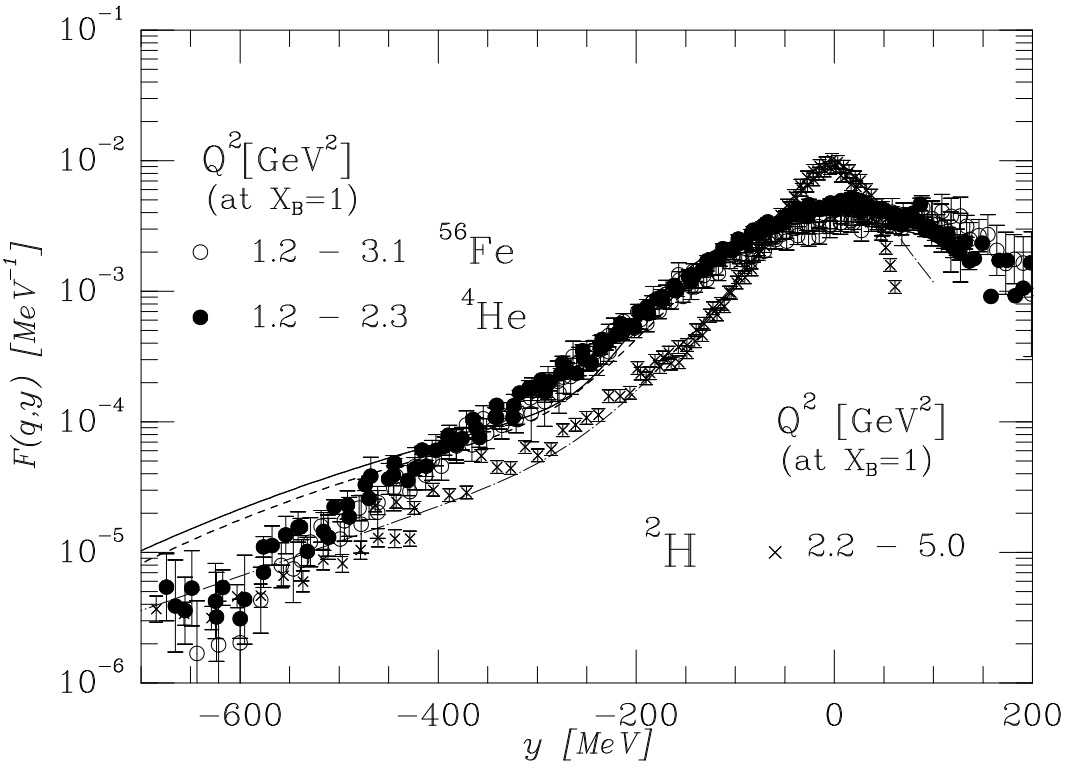

FIG. 2. The experimental scaling function of ^4He (solid circles) and ^{56}Fe (open circles) plotted *vs* the usual scaling variable y, compared to the scaling function of ^2H (crosses). The solid, dashed and dot-dashed curves represent the theoretical longitudinal momentum distributions of ^{56}Fe, ^4He and ^2H, respectively (after Ref.2) .

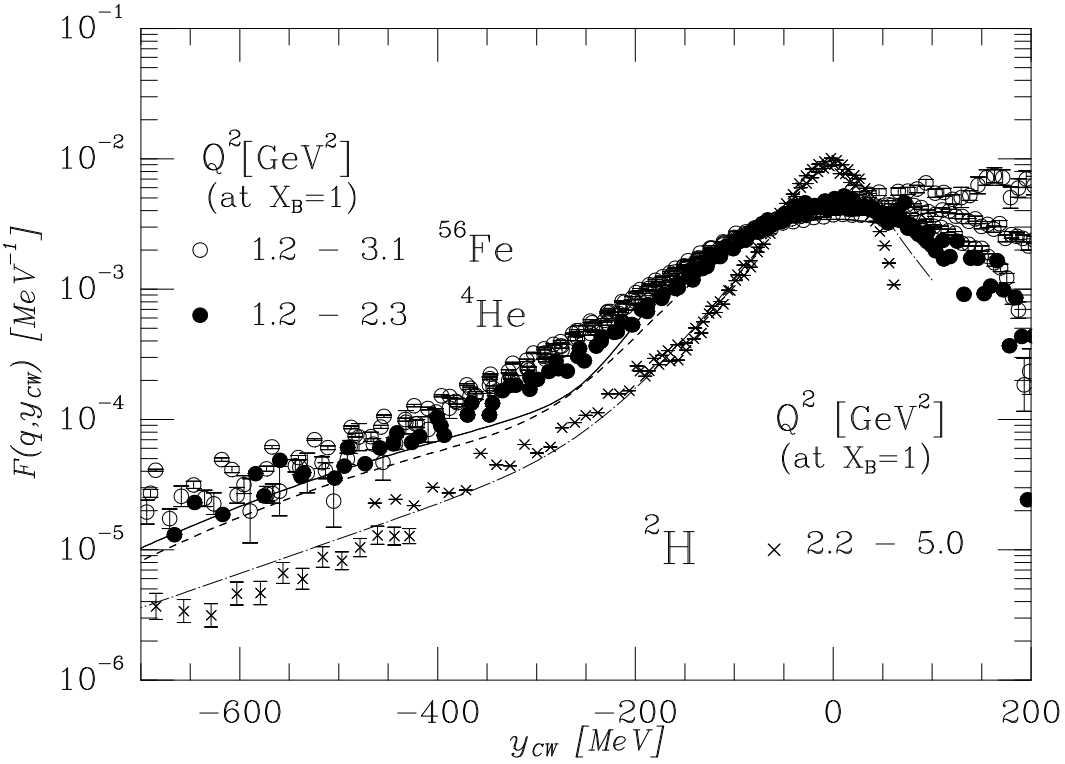

FIG. 3. The same as in Fig. 2 but plotted *vs.* y_{CW} as defined by Eq.(14), (after Ref.2)

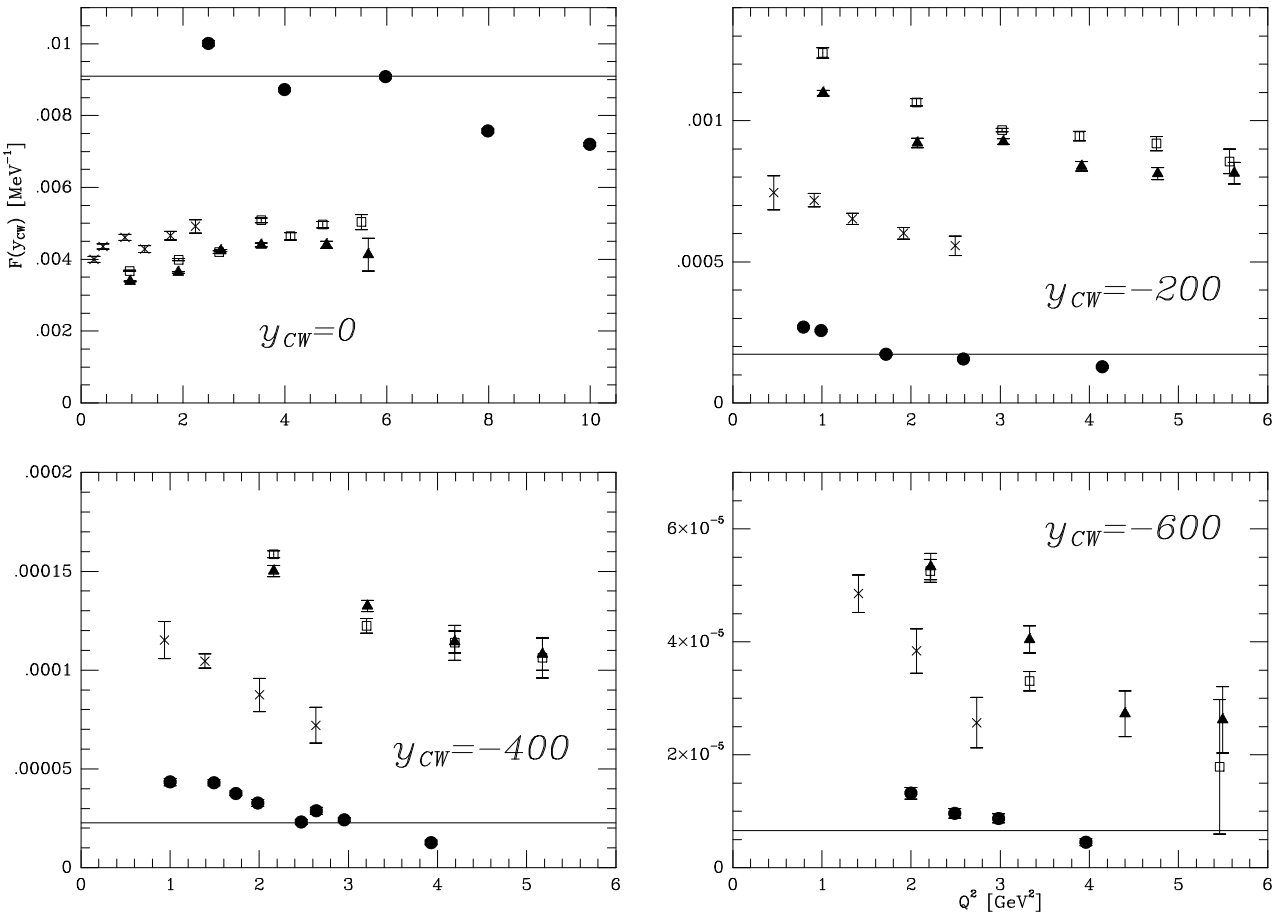

FIG. 4. The scaling functions of ^2H (solid circles), ^4He (crosses), ^{12}C (triangles) and ^{56}Fe (squares) at fixed values of y_{CW} plotted *vs* Q^2.

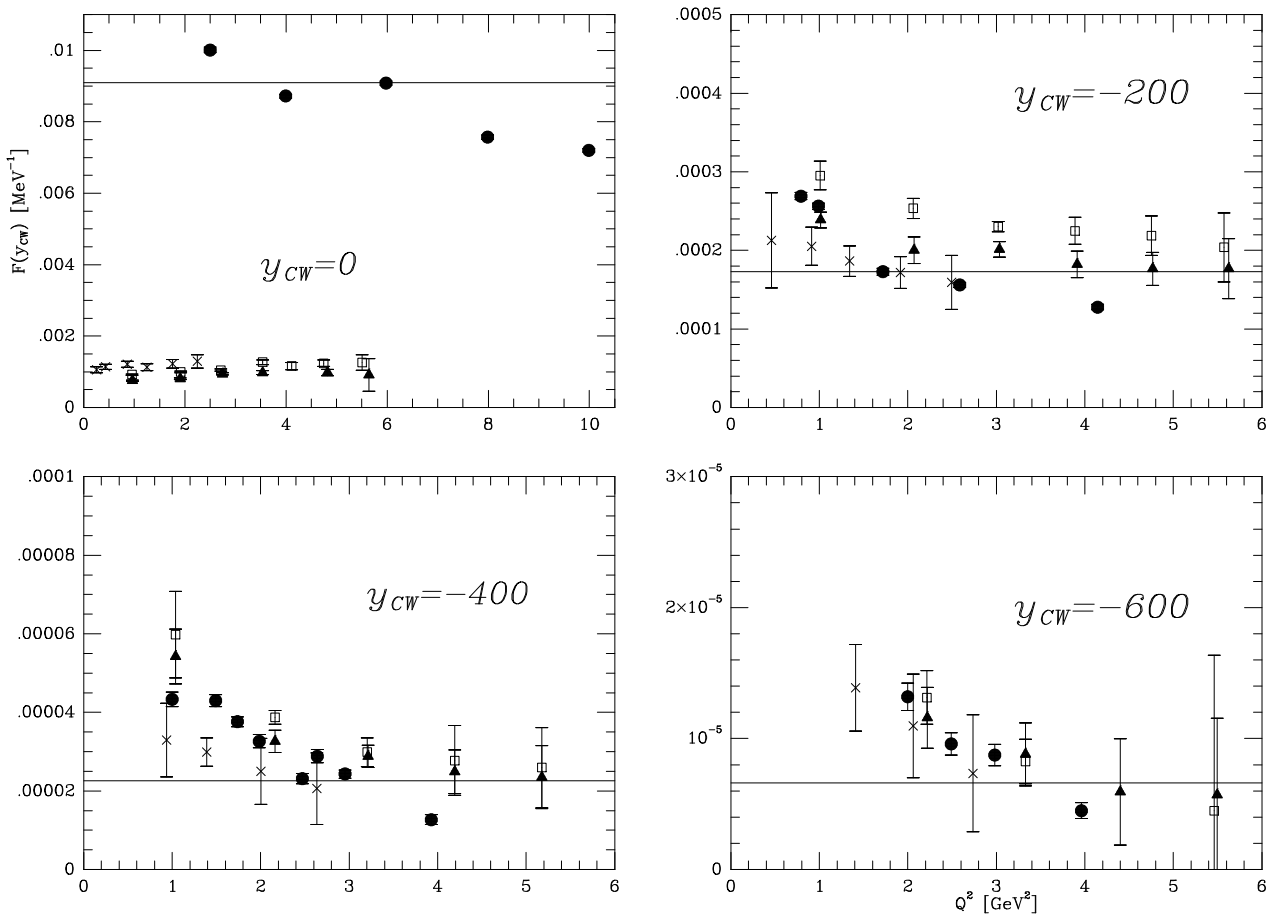

FIG. 5. The same as in Fig. 4 but with $F(y_{CW}, q)$ divided by the constant, C_A, defined in Eq. (17). The data exhibit a universal behaviour where the scaling function of any nucleus in a wide range of y_{CW} is simply C_A times that of the deuteron.

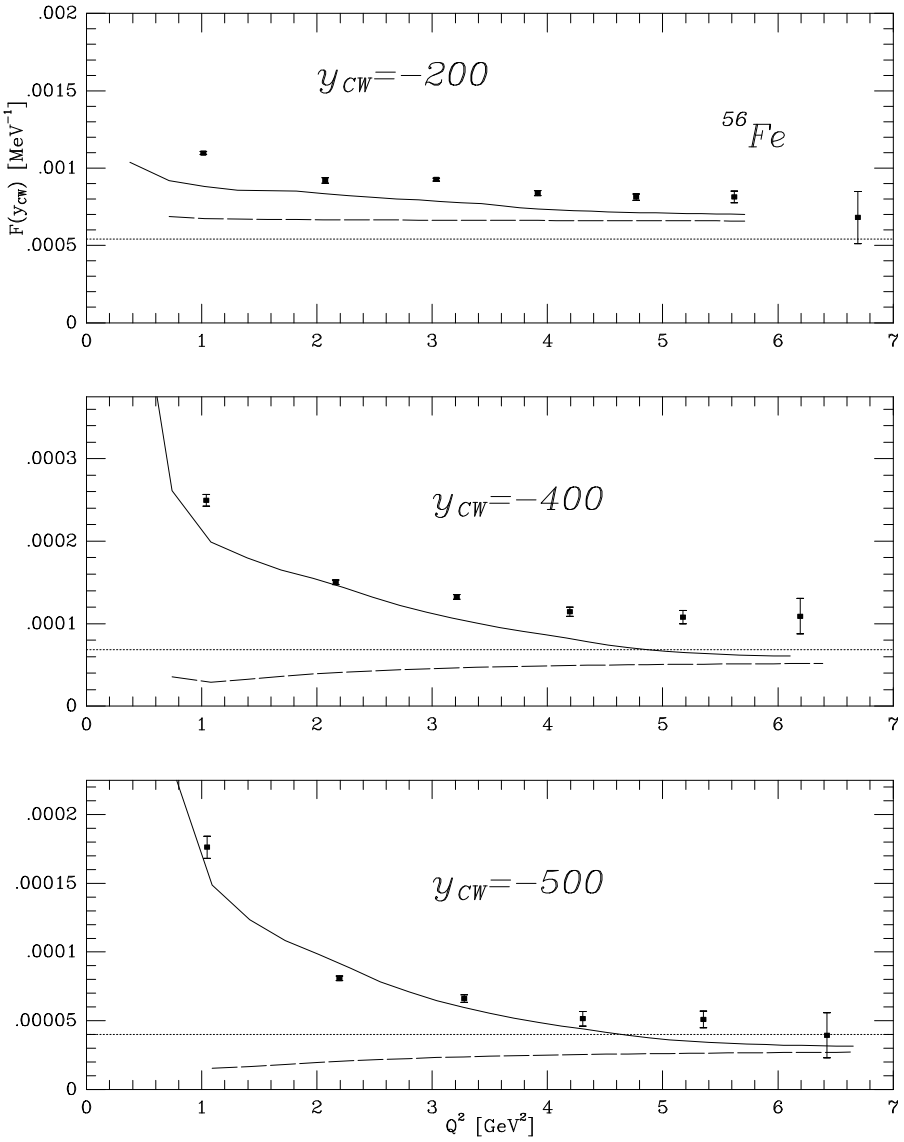

FIG. 6. The scaling function of ^{56}Fe *vs* Q^2 for fixed values of y_{CW} compared with the PWIA (dashed line) and the full FSI result (full line). The dotted line represents the longitudinal momentum distributions.

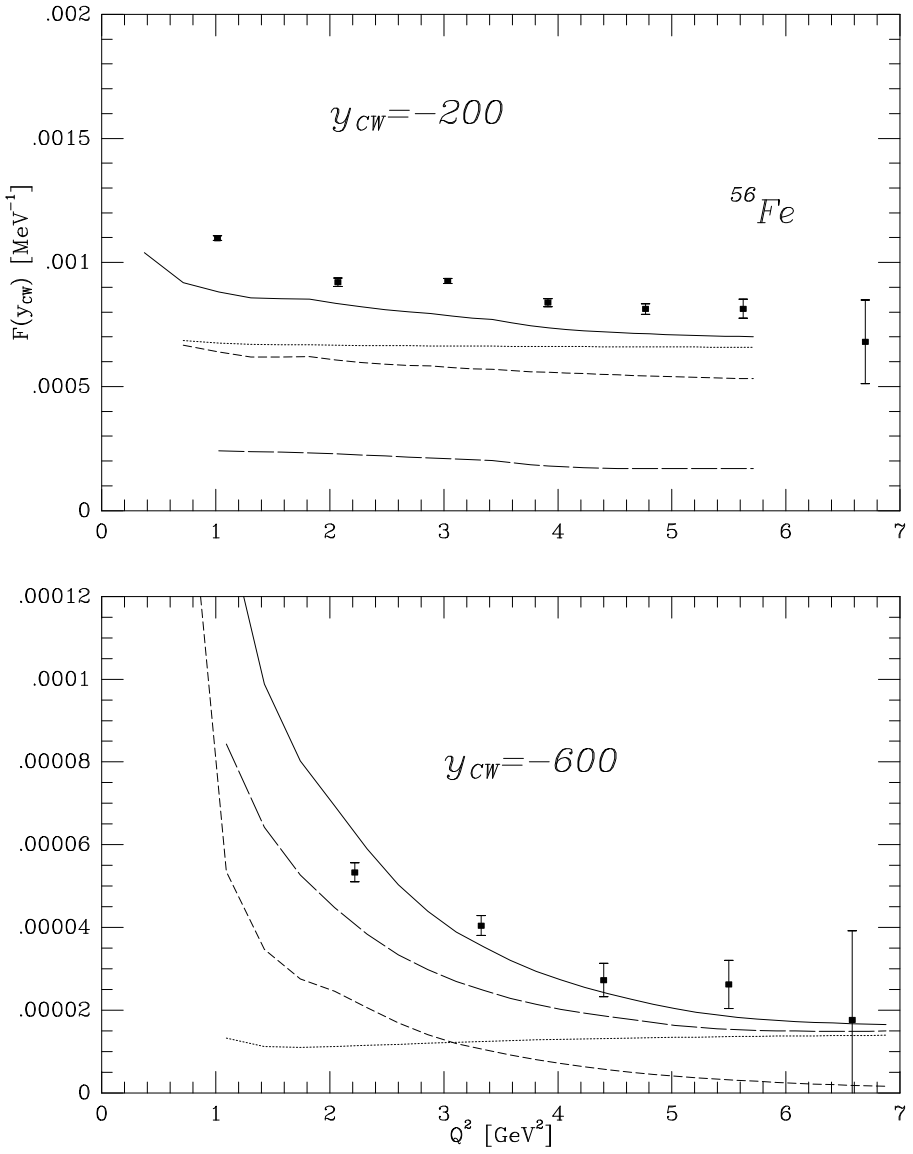

FIG. 7. The various contributions to the full FSI result (full curve): *PWIA*: dots; *optical potential*: short dashes; *two-nucleon rescattering*: long dashes.

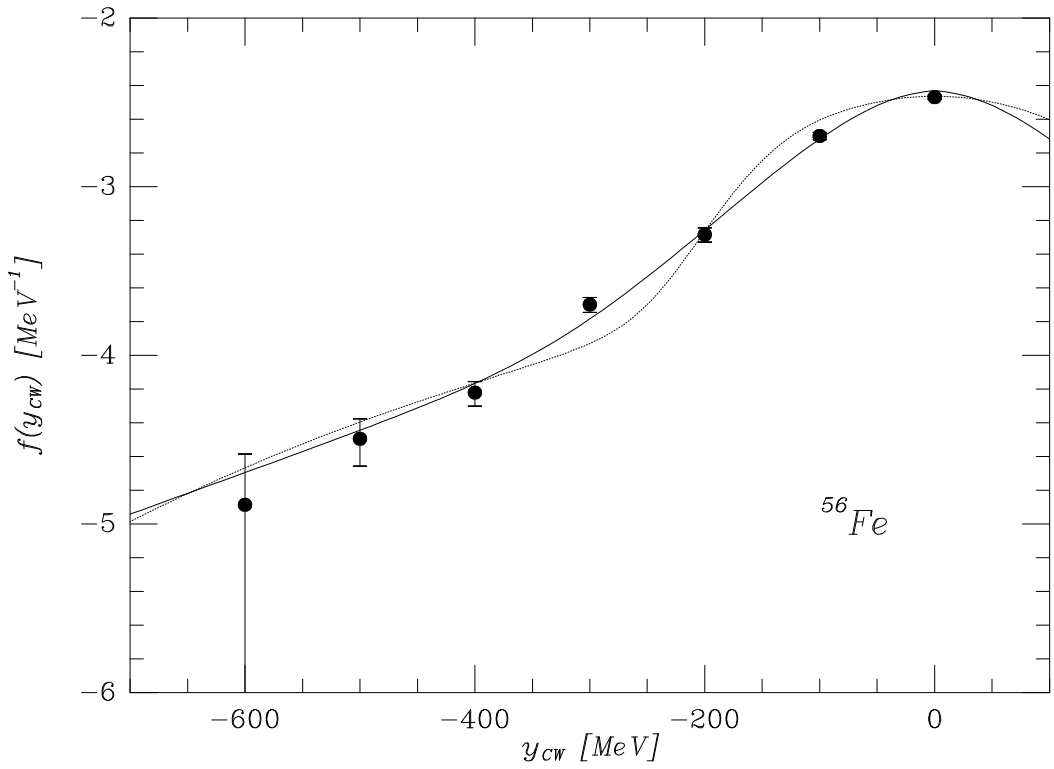

FIG. 8. The longitudinal momentum distribution (dots) for ^{56}Fe obtained from the results shown in Figs. 4-7. The dotted and solid curves correspond to two different theoretical longitudinal momentum distributions.